

Synthesis and Photoinduced Magnetic Properties of a Mn12 Single Molecule Magnet by the *cis-trans* Isomerism of Azobenzene

Sheby M. George and Jinkwon Kim*

Department of Chemistry, Kongju National University, Kongju, Chungnam 314-701, Korea. *E-mail: jkim@kongju.ac.kr
Received March 5, 2009, Accepted March 26, 2009

[Mn₁₂O₁₂(azo-L)₁₆(H₂O)₄] (**1**), a new Mn12 single molecule magnet containing a photochromic azobenzene ligand, has been successfully synthesized by substitution of acetate ligand of Mn12 with 6-[4-{4-hexyloxyphenyl(azo)}-phenoxy]hexanoic-1-acid. The reversible photoisomerization of the azobenzene group was confirmed by UV-visible absorption spectroscopy. The temperature and field dependence of dc susceptibility and the temperature and the frequency dependence of ac susceptibility were measured for the *cis* and the *trans* isomer of **1**. The magnetization value of the *cis* isomer in dc measurement is higher than that of the *trans* isomer. The *cis* isomer of **1** has a slower relaxation because *cis-trans* photoisomerization of the azobenzene group in peripheral ligands induces changes in its structure and dipole moment.

Key Words: Single-molecule magnets, Magnetic properties, Azobenzene, Photochromism, Mn12

Introduction

Optically switchable magnetic materials have become of quite substantial importance in the field of high-density information storage media.¹⁻³ One of the promising strategies to achieve photochemically active magnetic materials is to hybridize magnetic clusters with photochromic organic materials to control their properties by light illumination.⁴ The photoswitching of the hybrid materials can be induced as the electronic, and the magnetic properties of the photochromic organic materials are changed by structural distortion such as isomerization.⁵

There have been several attempts to control the magnetic properties of nanoparticles using photoresponsive ligands,⁶ but few attempts have been done with molecular magnetic clusters such as single molecule magnets (SMMs). The SMMs have been considered promising materials for future application in data storage and quantum computing⁷ because they have a very large coercive field, quantum tunneling of magnetization (QTM), and quantum phase interference.^{8,9} The best known examples of SMMs are the Mn12 clusters having the general formula of [Mn₁₂O₁₂(O₂CR)₁₆(H₂O)₄].¹⁰ In this paper, we report synthesis and magnetic characterizations of [Mn₁₂O₁₂(azo-L)₁₆(H₂O)₄] (**1**) containing an azobenzene group in its peripheral ligands.

Experimental

Materials. All chemicals were obtained commercially and used as received. All solvents used are of HPLC grade. [Mn₁₂O₁₂(O₂CMe)₁₆(H₂O)₄]·2CH₃COOH·4H₂O (Mn12ac) was prepared as reported.¹¹

Synthesis of Ligand (azo-L). The azo compound 6-[4-{4-hexyloxyphenyl(azo)}-phenoxy]hexanoic-1-acid was synthesized with a slight modification of the literature method.¹²

4-Hydroxy-4'-hexyloxyazobenzene. 4-(hexyloxy)-aniline (2.44 g, 12.6 mmol) was added to 3.2 mL of 12 M HCl in 10 mL distilled water and stirred at room temperature for 30 min.

The mixture was then cooled to 0 °C and a solution of NaNO₂ (0.869 g, 12.6 mmol) in 15 mL of distilled water was added drop by drop. To the resulting solution, was added phenol (1.98 g, 21.1 mmol) dissolved in 12.6 mL of 2 N NaOH drop wise. The yellow mixture was stirred for 2 h and the precipitate was filtered and dried in air. The product was further purified by column chromatography with hexane/ethylacetate (8:2) *R_f* 0.27. Yield 2.2 g (59%). ¹H NMR (CDCl₃) δ 7.84 (m, 4H), 6.9 (m, 4H), 5.36 (s, 1H), 4.03 (t, 2H), 1.8 (m, 2H), 1.47 (m, 2H), 1.36 (m, 4H), 0.93 (m, 3H).

6-[4-{4-Hexyloxyphenyl(azo)}-phenoxy]hexanoic-1-acid Methyl Ester. To a mixture of 4-hydroxy-4'-hexyloxyazobenzene (1 g, 3.36 mmol) and anhydrous K₂CO₃ (0.5788 g) in 100 mL of acetone was added 18C6 (0.16 g, 0.67 mmol) and 6-bromohexanoic acid methyl ester (0.7015 g, 3.36 mmol) in 50 mL acetone. The mixture was heated to reflux for 48 h and then solvent was evaporated. The residue was partitioned between dichloromethane-water solvents. Dichloromethane layer was collected and dried over Na₂SO₄. The yellow solid was purified by repeated precipitation from methanol until there was no impurity on TLC. Hexane/EtOAc (8:2), *R_f* 0.43. Yield 1.2623 g (88.2 %). ¹H NMR (CDCl₃) δ 7.84 (m, 4H), 6.9 (m, 4H), 4.01 (m, 4H), 3.66 (s, 3H), 2.34 (t, 2H), 1.8 (m, 4H), 1.65 (m, 2H), 1.45 (m, 4H), 1.3 (t, 4H), 0.9 (m, 3H).

6-[4-{4-Hexyloxyphenyl(azo)}-phenoxy]hexanoic-1-acid (azo-L). The ester was hydrolyzed using KOH at refluxing condition in THF/H₂O/EtOH mixed solvents until there was no ester on TLC. The solution was acidified with dilute HCl with pH of 4 or 5. The precipitate was collected by filtration. *R_f* 0.43 (Hexane/EtOAc (1:1)). ¹H NMR (DMSO-*d*₆) δ 7.8 (d, 4H), 7.09 (d, 4H), 4.07 (m, 4H), 2.5 (t, 4H), 2.25 (t, 2H), 1.75 (m, 4H), 1.6 (m, 2H), 1.45 (m, 4H), 1.34 (m, 2H), 0.88 (m, 3H).

Synthesis of [Mn₁₂O₁₂(azo-L)₁₆(H₂O)₄] (1**).** A slurry of Mn12ac (206 mg, 0.1 mmol) in dichloromethane (30 mL) was stirred with azo-L (680 mg, 1.65 mmol) for 4 h at room temperature. As the substitution progressed, all the reactants started to dissolve in solvent and finally to give a dark brown solution. Azeotropic distillation with toluene (20 mL) was

performed 9 times to remove completely the released acetic acid. The resulting dark brown residue was dissolved again in dichloromethane and treated with hexane. The crystalline solids were collected by filtration. FTIR data(KBr): 1599(s), 1580(s), 1500(s), 1467(m), 1420(m), 1393(m), 1316(w), 1296(w), 1247(vs), 1147(s), 1105(w), 1046(w), 1024(w), 936(w), 840(s), 727(w), 715(w), 669(w), 640(m), 612(w), 551(m). Calcd. for $C_{38.4}H_{50.4}O_{80}N_{32}Mn_{12}$ (Mw. 7507.5): C, 61.43; H, 6.77; N, 5.97. Found: C, 61.39; H, 6.71; N, 6.01.

Characterization. Variable-temperature magnetic susceptibility measurements were carried out on powder samples of the complexes using a Quantum Design MPMS-XL magnetometer equipped with a 50 kG magnet. The ac susceptibility data were collected in the frequency range of 20-1500 Hz at the ac field of 3 Oe. Corrections for the diamagnetism of the complexes were estimated using Pascal's constants, and magnetic data were corrected for diamagnetic contributions of the sample holder.

Elemental analysis was carried out by an Elementar vario EL III analyzer. Infrared spectra were recorded from KBr pellets with a Perkin-Elmer spectrum BX spectrophotometer. NMR spectra were recorded at VARIAN MERCURY400 spectrometer. Absorption spectra of the samples were measured on SCINCO S-4100 spectrophotometer using dichloromethane solutions of **1**. Photoisomerization of **1** was carried out in dichloromethane solution using a high-pressure Hg-Xe lamp (Oriel, 500 W) equipped with a UV35 band-pass filter and a sharp cut Y46 glass filter (Shimadzu Co.) for UV and visible light irradiation, respectively. The power densities of the incident light were adjusted to 10 mW/cm² for UV and 50 mW/cm² for visible light using an optical power meter (Melles Griot, 13PEM001).

Results and Discussion

Fig. 1 shows UV/Vis absorption spectra of **1** before and after UV or visible illumination for 5 min at room temperature. In general, azobenzene exhibits $\pi-\pi^*$ and $n-\pi^*$ transition bands at around 360 nm and at around 460 nm.

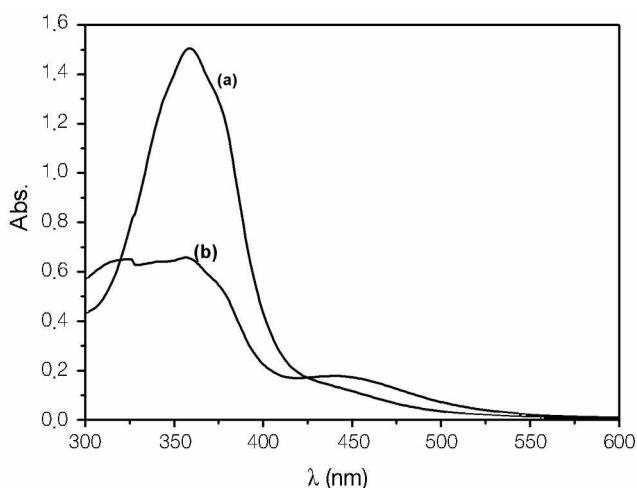


Figure 1. Changes in the UV-vis spectra of **1** up on illumination with UV for 5 min at room temperature. (a) is for the *trans* isomer and (b) is for the *cis* isomer.

respectively. After 5 min of UV illumination, the intensity of the peak at 360 nm decreased and the peak at 460 nm increased, indicating photoisomerization from *trans* to *cis*. After the subsequent illumination of visible light, the reverse process proceeded. The reversible *cis-trans* photoisomerizations were repeated several times by the alternating illumination of UV and visible light (Fig. 2).

The magnetic properties of the powder sample of **1** were studied using a SQUID magnetometer. Magnetic measurements were taken on the *trans* isomer first, and then the sample was irradiated with UV light of 360 nm for 5 min in solution phase and was then dried *in vacuo* under darkness and magnetic measurements were taken for the *cis* isomer.

Fig. 3 shows the ZFC-FC plots of the *trans* isomer (empty circle) and the *cis* isomer (filled circles) of **1**. Both isomers have a blocking temperature at around 3 K, but the magnetization value for the *cis* isomer is considerably higher than the *trans* isomer. The structural isomerism by UV illumination brings about changes in the dipole moment of the azobenzene moieties, which seem to have a direct effect on the magnetic properties of these materials.^{6b,6c,13} In general, the photo-

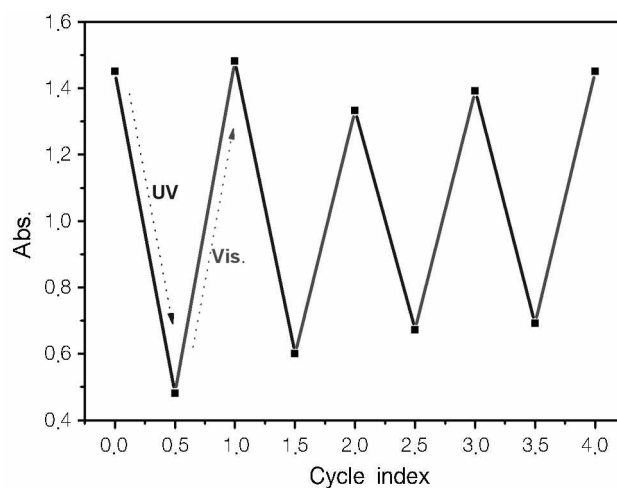


Figure 2. Plot of absorption at 360 nm showing the reversible *cis-trans* isomerism of **1**.

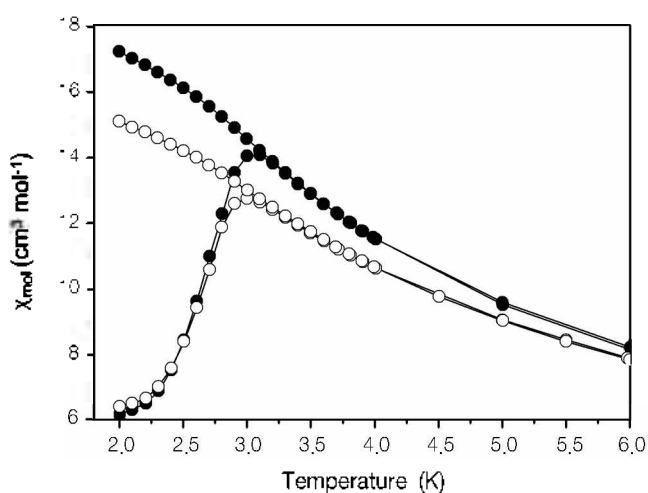


Figure 3. ZFC-FC plots of the *trans* (empty circles) and the *cis* (filled circles) isomer at 0.1 T.

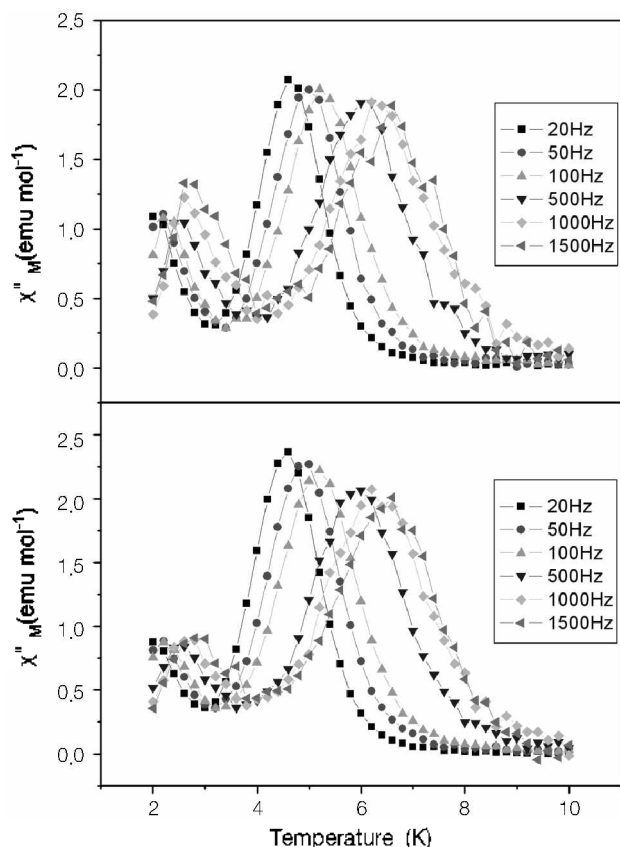


Figure 4. Temperature dependence of out of phase AC susceptibility signals of *trans* (above) and *cis* (below) form of **1**.

isomerization of the azobenzene derivatives, particularly the *trans*-to-*cis* isomerization reaction, is accompanied by an increase in molecular volume.^{6c} Previous magnetic study on the organic-inorganic hybrid material composed of Mn12ac and azobenzene in PMMA shows no significant change in dc susceptibility upon light illumination. It is mainly due to the structural change in solid matrix is less plausible.¹⁴ Furthermore, in this composite contribution of electromagnetic field between Mn12ac and azobenzene may be negligible because there are no direct chemical bonds between them.¹⁵

Out-of-phase ac magnetic susceptibility (χ''_M) measurements were carried out in the region of 2 to 10 K at the zero dc field. As displayed in Fig. 4, both isomers predominantly show a peak in the 4–7 K region with a smaller peak in the 2–4 K. However, the peak in the lower temperature region becomes weaker as the *trans* isomer is converted into the *cis* isomer. Illumination of UV light brought down the intensity ratio of the lower temperature peak to that at the higher temperature peak from 1:2 to 1:2.5. Peak maxima are accurately determined by fitting the peaks to a Lorentzian function. A least-squares fit of ac susceptibility relaxation data to Arrhenius equation gives $U_{\text{eff}} = 68.88$ K for the *trans* isomer and $U_{\text{eff}} = 72.1$ K for the *cis* isomer. If two isomers have the same core geometry and the same ground spin, the main origin for the different relaxation rates may be different transverse magnetic fields by dislocations. The local rotations of the easy axis due to dislocations result in a transverse

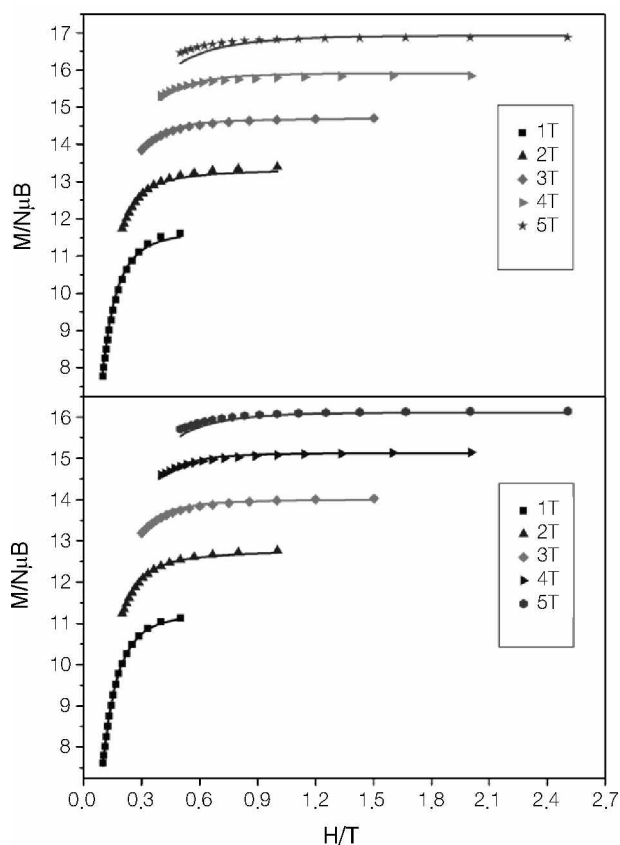


Figure 5. Plot of $M/N\mu_B$ vs H/T for the *cis* (below) and the *trans* (above) form of **1** at indicated applied fields. The solid lines are fits of the data.

magnetic field for an external field applied along the *c* axis of the crystal.^{16,17} The *trans* isomer might have a higher transverse anisotropy and field than those of the *cis* isomer.

Plots of reduced magnetization ($M/N\mu_B$) as a function of H/T , where N is Avogadro's number and μ_B is the Bohr magneton, were also obtained for the both isomers of **1** (Figure 5). The data were fitted to the basic thermodynamic expression given in Equation (2), which takes the full power of the average of the magnetization into account.¹⁸

$$M = -\frac{N}{4\pi} \int_0^{2\pi} \int_0^\pi \frac{\sum_P (dE_P/dH) \exp(-E_P/k_B T)}{\sum_P \exp(-E_P/k_B T)} \times \sin\theta d\theta d\phi \quad (2)$$

In Equation (2), k_B is the Boltzmann constant and E_P is the eigenenergy obtained by diagonalization of the spin Hamiltonian matrix, including axial zero-field splitting and Zeeman interactions. The data were fitted using ANISOFIT¹⁹ to give $S = 10$, $g = 1.97$, $D = -0.31$ cm⁻¹, and $E = 0.0009$ cm⁻¹ for the *trans* isomer while $S = 10$, $g = 1.93$, $D = -0.34$ cm⁻¹, and $E = 0.0004$ cm⁻¹ for the *cis* isomer, where D is the axial zero field splitting parameter and E is the rhombic zero field splitting parameter. The *cis* isomer has a larger uniaxial anisotropy than the *trans* isomer, which is consistent with the observation in ac susceptibility measurements.

Figure 6 shows the M-H hysteresis loop of the *cis* and *trans*

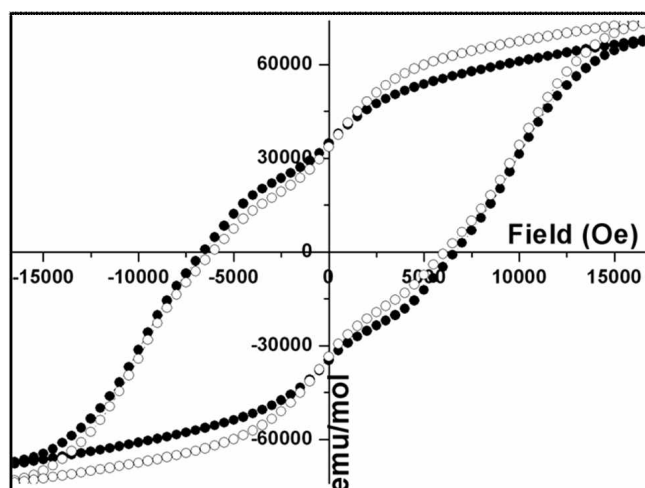


Figure 6. M-H hysteresis loop of the *trans* (empty circles) and *cis* (filled circles) isomers of **1** at 2 K.

isomers of **1**. Small plateaus for both the isomers are observed in the hysteresis loop because of quantum tunneling of magnetization. The *cis* isomer shows a larger coercive field (H_c) compared to the *trans* isomer. The difference in the coercive field is about 518 Oe, indicating a faster relaxation of the *trans* isomer.

The physical phenomena exhibited by the Mn12, like SMMs, are readily affected by the small changes in its molecular structure. The *trans*-to-*cis* photoisomerization of the azobenzene is usually accompanied by an increase in its molecular volume. This change induces a large structural change in the molecular arrangement, which leads to changes in its magnetic properties. The slow relaxation shown by the *cis* form compared to the *trans* is an overall result of change in the change in packing and structural rearrangement caused by the azobenzene group with UV illumination. The nature of the azobenzene group to occupy large volume in its *cis* form rather than the well-packed *trans* form may also result in an increase in the intermolecular distance of Mn12.

In summary, we successfully synthesized new Mn12 SMM which carries photo responsive ligands and responds to the UV-vis illumination with a significant change in its properties.

Acknowledgments. This work was supported by the Ministry of Education, Science and Technology (Grant no. M1030000023405J000023410). S. M. George is thankful to KRF for research fellowships.

References

1. Kuch, W. *Nat. Mater.* **2003**, *2*, 505.
2. Thirion, C.; Wernsdorfer, W.; Mailly, D. *Nat. Mater.* **2003**, *2*, 524.
3. Gullich, P.; Garcia, Y.; Woike, T. *Coord. Chem. Rev.* **2001**, *219-221*, 839.
4. Einaga, Y. *Bull. Chem. Soc. Jpn.* **2006**, *79*, 361.
5. Irie, M. *Chem. Rev.* **2000**, *100*, 1683.
6. (a) Nakatani, K.; Yu, P. *Adv. Mater.* **2001**, *13*, 1411. (b) Einaga, Y.; Yamamoto, T.; Sugai, T.; Sato, O. *Chem. Mater.* **2002**, *14*, 4846. (c) Mikami, R.; Taguchi, M.; Yamada, K.; Suzuki, K.; Sato, O.; Einaga, Y. *Angew. Chem., Int. Ed.* **2004**, *43*, 6135. (d) Taguchi, M.; Yamada, K.; Suzuki, K.; Sato, O.; Einaga, Y. *Chem. Mater.* **2005**, *17*, 4554.
7. Gatteschi, D.; Sessoli, R. *Angew. Chem., Int. Ed.* **2003**, *42*, 268.
8. Friedman, J. R.; Sarachik, M. P.; Tejada, J.; Ziolo, R. *Phys. Rev. Lett.* **1996**, *76*, 3830.
9. Wernsdorfer, W.; Chakov, N. F.; Christou, G. *Phys. Rev. Lett.* **2005**, *95*, 147201.
10. Mertes, K. M.; Suzuki, Y.; Sarachik, M. P.; Myasoedov, Y.; Shtrikman, H.; Zeldov, E.; Rumberger, E. M.; Hendrickson, D. N.; Christou, G. *Solid State Commn.* **2003**, *127*, 131.
11. Lis, T. *Acta Cryst.* **1980**, *B36*, 2042.
12. Wei, W.-H.; Tomohiro, T.; Kodaka, M.; Okuno, H. *J. Org. Chem.* **2000**, *65*, 8979.
13. (a) Yamamoto, T.; Umemura, Y.; Sato, O.; Einaga, Y. *Chem. Mater.* **2004**, *16*, 1195. (b) Einaga, Y.; Sato, O.; Iyoda, T.; Fujishima, A.; Hashimoto, K. *J. Am. Chem. Soc.* **1999**, *121*, 3745.
14. Akitsu, T.; Nishijo, J. *J. Magn. Magn. Mater.* **2007**, *315*, 95.
15. Akitsu, T. *J. Magn. Magn. Mater.* **2009**, *321*, 207.
16. Garanin, D. A.; Chudnovsky, E. M. *Phys. Rev. B* **2002**, *65*, 94423.
17. (a) Jeon, W.; Jin, M. K.; Kim, Y.; Jung, D.-Y.; Suh, B. J.; Yoon, S. *Bull. Korean Chem. Soc.* **2004**, *25*, 1036. (b) Lim, J. M.; Do, Y.; Kim, J. *Bull. Korean Chem. Soc.* **2005**, *26*, 1065.
18. Vermaas, V.; Groeneveld, W. I. *Chem. Phys. Lett.* **1974**, *27*, 583.
19. Shores, M. P.; Sokol, J. J.; Long, J. R. *J. Am. Chem. Soc.* **2002**, *124*, 2279.